

# Computational Studies: Cisplatin

Yogita Mantri and Mu-Hyun Baik

Indiana University, Bloomington, IN, USA

---

1	Introduction	1
2	Mode of Action of Cisplatin	1
3	Structural/Cellular Responses to Cisplatin DNA Binding	2
4	Modeling Cisplatin–DNA Complexes	2
5	Small Models	3
6	Large Models	8
7	Related Studies	11
8	Concluding Remarks	13
9	Abbreviations and Acronyms	14
10	References	14

---

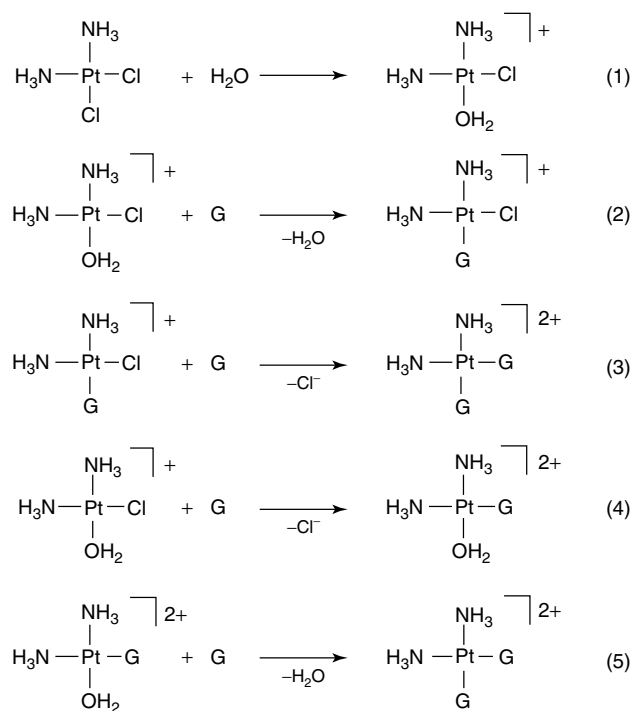
## 1 INTRODUCTION

Cis-diamminedichloroplatinum(II), cisplatin, is a potent anticancer drug that has been in clinical use for three decades.<sup>1–4</sup> It was accidentally discovered by Rosenberg while examining the influence of electric current on bacterial growth.<sup>5–7</sup> Following extensive testing, cisplatin was FDA approved in 1978.<sup>8</sup> Since then, it has become one of the most widely used anticancer drugs, especially in the treatment of testicular, ovarian, head-and-neck and small-cell lung cancers, as well as several other types of cancers in combination with other drugs.<sup>9,10</sup> Despite being remarkably successful, there are a number of unsolved problems associated with this drug that limit its value in clinical use, the most important being the following: severe side effects, its ineffectiveness against several types of common cancers, and natural and acquired resistance displayed by a significant number of patients.<sup>11,12</sup> In recent decades much effort was devoted to finding analogs with improved efficacy and reduced toxicity.<sup>13,14</sup> The search for analogs however, has so far yielded disappointingly few candidates that have reached clinical use, namely, oxaliplatin, nedaplatin, and carboplatin.<sup>15–17</sup> This modest success at discovering new drugs through screening and experimental trials alone highlights the need for a more rational approach. Whereas the general mode of action is agreed upon, many details about how cisplatin interacts with its cellular target, genomic DNA, remain poorly understood. Computational

studies can offer valuable insights and possibly provide a foundation for new strategies.

## 2 MODE OF ACTION OF CISPLATIN

Cisplatin is administered intravenously, and remains in its neutral form in the bloodstream and extracellular medium. The cellular uptake occurs by passive diffusion across the membrane or actively by membrane transport proteins, in particular by the copper transporter Ctr1.<sup>8,9,18</sup> Inside the cell, the sudden decrease in the chloride concentration from  $\sim 100$  mM to  $\sim 4$  mM causes hydrolysis and chloride dissociation to form the activated complexes *cis*-diamminechloroaquaPt(II) and *cis*-diamminediaquaPt(II) (Scheme 1).<sup>19</sup> Presumably, these positively charged complexes are electrostatically attracted to the negatively charged DNA and eventually form stable adducts at the N7 positions of purine bases, in particular guanine.<sup>9,20,21</sup> Because cisplatin contains two labile ligands, it can lose both chlorides and form bifunctional adducts. These adducts distort DNA such that polymerases are stalled at the site of platination (Figure 1), resulting in an interruption of replication and transcription that ultimately triggers the cascade of events involved in apoptosis or cell-death.<sup>22,23</sup>



Scheme 1

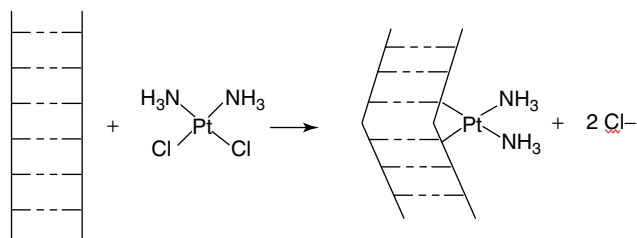


**Figure 1** Schematic of distortion of DNA structure upon cisplatin binding

### 3 STRUCTURAL/CELLULAR RESPONSES TO CISPLATIN DNA BINDING

Cisplatin prefers to bind to guanine over adenine and the major adducts detected typically are 1,2-intrastrand GpG crosslinks (~67%),<sup>24</sup> followed by 1,2-intrastrand ApG crosslinks (~10%).<sup>25,26</sup> 1,3-intrastrand crosslinks of two guanine bases are also found as a minor product. Other binding modes include monofunctional binding, interstrand crosslinks and DNA-protein crosslinks. The intrastrand crosslink causes a substantial kink in the DNA helix axis in the range of 30–80°, depending on the experimental conditions,<sup>9</sup> presumably causing polymerase activity to be interrupted. The intrastrand crosslinks are possible only in cisplatin, and not transplatin where the ammine groups are bound trans to each other. Transplatin preferentially forms monofunctional

adducts or makes interstrand crosslinks. Because the cytotoxic activity of transplatin is much less pronounced than what is seen for cisplatin, this binding difference is taken as strong evidence that the mode of action requires intrastrand crosslinks with DNA.

Among the many disadvantages of cisplatin, the most crucial problems that have fueled an intensive search for analogs are the ineffectiveness against certain tumor types and its severe toxicity, in particular, nephrotoxicity. This search has, over the course of three decades, led to hundreds of lead compounds, only a handful of which reached clinical trials. During this exercise over the years, important lessons about the key features that comprise an effective Pt(II)-based drug have emerged. For example, structure-activity relationship studies had shown that at least one primary or secondary amine is needed for cytotoxic activity. Subsequent high resolution structural data of some of these candidates elucidated the role of the amine protons in forming stabilizing hydrogen bonds. To enable truly rational drug design, however, a detailed understanding of the atomic details of cisplatin activation and interactions with DNA, as well as other cellular components, is key. The use of computational modeling efforts can and have provided valuable insights that are far more challenging to obtain from other structural methods like NMR spectroscopy and X-ray crystallography.

Recent studies that have taken into account cellular responses to cisplatin suggest that simply binding the drug candidate strongly to DNA is not sufficient for pharmacological activity. Current consensus points to excision repair of the Pt-induced lesion being the main reason for inactivity of potential Pt-drugs. There is increasing awareness now that one important reason for cisplatin's performance is related to the high mobility group (HMG) proteins that bind to DNA and protect the drug–DNA adducts against excision repair (Figure 2).<sup>4</sup>

### 4 MODELING CISPLATIN–DNA COMPLEXES

Computational studies have complemented experimental efforts to understand almost every step of the mode of action of cisplatin, from hydrolysis to activate the drug to the binding of repair proteins with the final adducts. The combination of dramatically improved computer hardware and robust, sophisticated, and numerically efficient modeling software has allowed for employing high levels of theory to examine various aspects of cisplatin chemistry using computational chemistry techniques. The studies reviewed in this chapter are organized into three sections—the first deals with small models to probe the detailed electronic structure of cisplatin and its interactions with free purine bases, the second covers studies on cisplatin adducts with larger models of DNA and the dynamics of cisplatin–DNA complexes, and the last

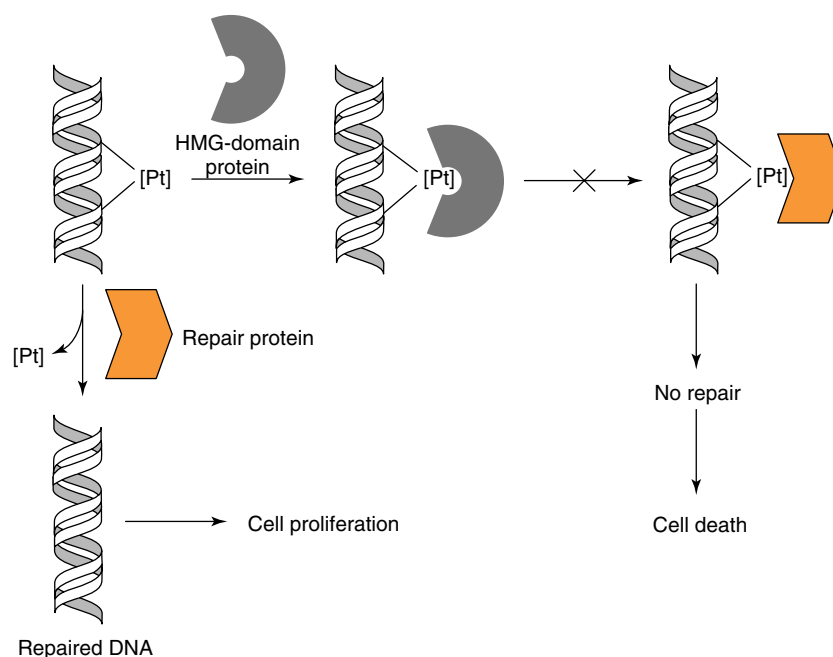


**Figure 2** Repair of cisplatin–DNA adducts

section covers related complexes including other platinum- and nonplatinum-based anticancer agents.

## 5 SMALL MODELS

The very first computational studies on cisplatin aimed to better understand the hydrolysis of cisplatin, because the activation by hydrolysis had long been established as the rate-limiting step. In addition, studies were also performed on general substitution reactions in cisplatin and related Pt(II) complexes, to understand and better tune the reactivity in cisplatin analogs in general. Several studies also dealt with a comparison of cisplatin binding to the purine bases guanine and adenine to explain the greater preference for forming adducts with guanine. Finally, the reactivity differences between cis- and transplatin have been studied.

The introduction of relativistic effective core potentials (ECP) for transition metals, and in particular, benchmark studies comparing the geometries and bond energies of complexes of the type  $\text{Pt(II)(N/PH}_3)_2\text{XY}$  with experimental data,<sup>27,28</sup> laid the foundation for the reliable use of quantum mechanical methods for studying cisplatin chemistry. An intriguing question had been the preferential antitumor activity of the cis isomer over the trans isomer, a fact then attributed to the steric effects of binding DNA bases. It was eventually discovered that the cis orientation of the leaving groups allowed binding of two adjacent guanine bases on the same strand, which resulted in a large kink in the

DNA helix, causing polymerases to be stalled at the kink. In one of the earliest theoretical studies, Krauss *et al.* used density functional theory (DFT) to understand the barrier for cis–trans isomerization in cisplatin and related compounds, including the aqua and hydroxy derivatives that are formed upon cisplatin hydrolysis.<sup>29</sup> This work demonstrated that the trans isomer is favored over the cis isomer in all cases due to reduction in ligand–ligand repulsion, especially in the case of anionic ligands; however, these differences become negligibly small when favorable hydrogen bonding interactions are possible between the ammine ligands and the other labile ligands. Moreover, although the trans isomer is more stable than the cis isomer, the barrier for interconversion is high enough that isomerization will not occur at any reasonable rate. The same group subsequently reported one of the first *ab initio* model studies of the binding of cisplatin to nucleobases.<sup>30</sup> To enable comparison of the binding of Pt(II) to various positions in the four nucleobases in DNA and to keep computational costs to a minimum, the authors used  $\text{Pt(NH}_3)_3^{2+}$  as the fragment that interacted with the bases. The ranking of the bases followed the order:  $\text{G(N7)} > \text{C(N3)} > \text{C(O2)} > \text{G(O6)} > \text{A(N3)} \approx \text{A(N1)} > \text{A(N7)} > \text{G(N3)} > \text{T(O4)} > \text{T(O2)}$ , based on differential Pt(II) binding energies. The bidentate binding of the  $\text{Pt(NH}_3)_2^{2+}$  fragment to the N7 and O6 position of guanine was also calculated and found to be unfavorable. On the basis of the ranking above and the fact that most of the potential binding sites are in reality unavailable for binding due to Watson–Crick base pairing, the N7 position of guanine—in particular intrastrand binding to two adjacent guanines—was confirmed as the preferred binding site, in full agreement with experimental evidence.

Surprisingly, no new studies were reported for almost a decade following that work. In 1995, Parrinello *et al.* provided new insights into the structure and reactivity of cis- and transplatin and related hydrolysis products using DFT.<sup>31</sup> Their work benchmarked the application of DFT using the gradient-corrected-local density approximation exchange and correlation functionals to Pt(II) complexes. The wealth of available structural and spectroscopic data up to that point allowed a calibration of the theoretical protocol. In the same year, the same group reported another study using DFT to compare the electronic structures of cisplatin and its second-generation analog carboplatin.<sup>32</sup> Those results suggested that the replacement of the chloride ligands of cisplatin by carboxylate ligands in carboplatin resulted in a greater stability of the metal-ligand bonds in the latter, leading to a potentially higher activation energy for substitution reactions. However, the authors correctly point out that such predictions cannot be made realistically using only gas phase calculations because solvation effects are likely to play an important role. A more comprehensive study comparing the geometric, electronic, and vibrational properties of cisplatin using different basis sets, including pure ECP and hybrid ECP with various electron correlation methods up to the MP4 level, and DFT, was performed by Hausheer *et al.*<sup>33</sup> A more recent paper by Wysokinski *et al.* benchmarked the performance of various density functionals in calculating the structures and vibrational spectra of cisplatin and carboplatin,<sup>34</sup> concluding that the mPW1PW method and the ECP in the LanL2DZ basis set give results in better agreement with experiment, compared to the MP2 method. The inclusion of more elaborate ECP or larger basis sets did not significantly improve performance. These benchmarking studies thus laid the foundation for the application of computational methods toward solving chemical questions in the cisplatin field.

The rate-limiting step in the reaction of cisplatin with DNA is its hydrolysis to form activated chloroaqua and diaqua complexes. Thus, the hydrolysis reaction of cisplatin and other model complexes attracted much attention. For example, Nikolov *et al.* studied the thermodynamics of hydrolysis of

cisplatin and bis(ethylenediamine)dichloroplatinum(II) using a combination of molecular mechanics for obtaining optimized geometries of the reactants and products, and the extended Hückel method for deriving charge distributions and electronic energies.<sup>35</sup> A significant improvement in the study of reaction dynamics in solution phase was made by the introduction of Car-Parrinello molecular dynamics (CPMD), in which the interatomic forces are derived by ab initio calculations at the DFT level, thus allowing bond-forming and bond-breaking events to be modeled, which are not possible using classical force-fields. Using this approach, Andreoni *et al.* studied the kinetics of the first hydration step of cisplatin going to the mono-aqua complex. The transition state showed the characteristic trigonal bipyramidal geometry of associative ligand-substitution reactions (Figure 3), giving an activation barrier of 21 kcal mol<sup>-1</sup> that was very close to experimental estimates of 24–25 kcal mol<sup>-1</sup>.<sup>36</sup> To demonstrate the robustness of the method, a short timescale simulation was also performed on the GpG adduct formed between cisplatin and DNA in water.

The hydrolysis of cisplatin was studied by several others using various levels of theory, where a common approach adopted has been to use DFT to optimize the geometries of the key intermediates and reevaluate their energies using higher level ab initio methods, and/or adding solvation corrections based on continuum dielectric models.<sup>37–42</sup> One of the key characteristics of a drug that determines its efficacy is its uptake profile by cells. Although cisplatin is a neutral compound, it is fairly hydrophilic and is capable of forming hydrogen bonds with water. This hydrophilicity presents a challenge to uptake, in particular for highly hydrophobic cellular environments such as the intestines. To characterize where cisplatin fell in the Abraham scale of H-bond acidity/basicity, Robertazzi *et al.* applied the atoms-in-molecules (AIM) scheme using DFT to measure the thermodynamics of hydrogen bond formation, solvation, and hydrolysis of cisplatin in various environments.<sup>43</sup> More general studies on S<sub>N</sub>2 substitution reactions, and in particular hydration reactions, in square-planar Pt(II) complexes were

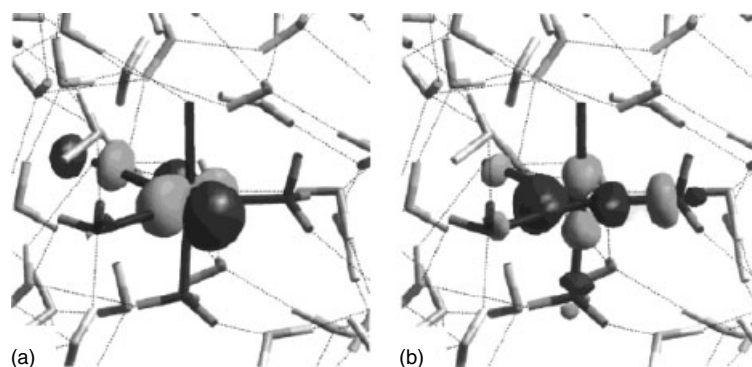


**Figure 3** HOMO (a) and LUMO (b) of the structure of the transition state for cisplatin hydrolysis, modeled by CPMD simulations. (Reproduced from Ref. 36. © ACS, 2000.)

also carried out. We mention these studies only in passing, as they are outside the scope of the current topic.<sup>44–46</sup>

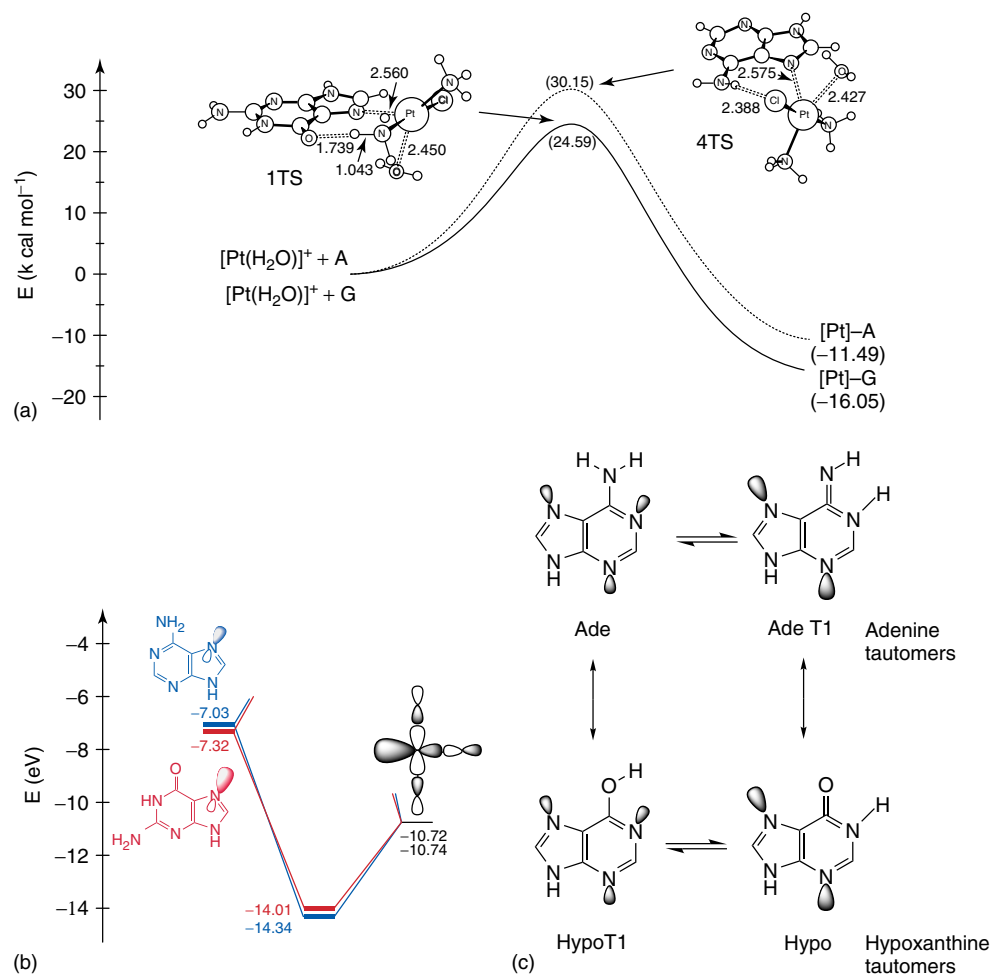
The work of Burda and Leszczynski represents a new class of complex calculations that have become possible using the new generation of computer hardware. These studies aimed at addressing structural issues such as the binding of cisplatin to a nucleotide or larger fragments of DNA that could not be addressed with minimalistic models. One representative paper describes the interaction of transplatin and the fragments *trans*-PtCl<sub>2</sub>(NH<sub>3</sub>)<sup>+</sup> and Pt(NH<sub>3</sub>)<sub>3</sub><sup>2+</sup> with G:C and A:T base pairs using DFT, followed by an MP2-based energy analysis.<sup>47</sup> In all cases, there is substantial contribution to the total binding energy by hydrogen bonding between an ammine ligand on Pt(II) and the exocyclic substituent of the purine base. Surprisingly, the Watson–Crick base-pairing between the base-pair G:C is found to become stronger upon platinum binding at the N7 position due to polarization effects, provided the platinum moiety is charged. This is somewhat surprising, as adding a hydrogen bond donor that interacts with the exocyclic oxygen may be expected to lead to a weakening of the hydrogen bond strength between the base pairs. In case of neutral platinum, there is no such strengthening for either base pair, and the effect of binding is the same as that of the cations like Zn<sup>2+</sup> and Mg<sup>2+</sup> that normally bind to the major groove.

A comparison between cisplatin and its nickel analog, cisnickel, both in terms of the structure and energetics of the isolated complexes and bound to G:C base pairs,<sup>48</sup> revealed that while the overall geometries and binding energies are comparable, the cisnickel complex has a much higher barrier for the cleavage of the M–Cl bond, suggesting that the nickel analogs may not be clinically useful because the hydrolysis step is rate limiting. Burda *et al.* also published work using MP2 and coupled cluster methods to study the hydration of cis- and transplatin and their Pd analogs, finding activation energies that were qualitatively in agreement with experiments.<sup>38</sup> For a deeper understanding of the crosslinks that constitute the majority of cisplatin–DNA adducts, namely, the GpG and ApG crosslinks, a comprehensive study was carried out surveying the thermodynamics of Pt-bridged complexes using combinations of adenine and guanine.<sup>49</sup> In agreement with experimental observations, the GG crosslink was found to be most preferred thermodynamically, followed by the AG crosslink. The greater preference was traced to greater Coulombic stabilization of the GG complex by intramolecular hydrogen bonding with the O6 oxo of guanine. In case of the GG crosslink, two such hydrogen bonds are present leading to greater preference compared to the cases involving adenine, which is only capable of weaker hydrogen bonds due to its amine exocyclic functional group. In a more recent study,<sup>50</sup> the stabilities of Pt-bridged bifunctional complexes using various combinations of the bases adenine, guanine, and cytosine, in the head-to-head and head-to-tail orientations were examined, revealing that the G–Pt–G complexes were the most preferred, followed by the G–Pt–C complexes. The adenine complexes

were found to be ~15 kcal mol<sup>-1</sup> higher in energy compared to the G–Pt–G complex, in keeping with the observed preference for formation of G–Pt–G complexes. While these calculations suggested that crosslinks involving cytosine is energetically also possible, in reality, the N3 position of cytosine is engaged in Watson–Crick base-pairing, and thus unavailable for binding platinum. The Platts group also used DFT to study the role of hydrogen bonding in the binding of cisplatin to G:C and A:T base pairs.<sup>51</sup> Their AIM treatment showed that hydrogen bonding is ubiquitous in all such complexes, and that differences in hydrogen bonding patterns alone could not account for the preference for guanine over adenine. In apparent contradiction with another study, their results showed that platinum binding weakened the Watson–Crick hydrogen bonds, resulting in distortions from the normal base-pair geometries.

Our own work sought to shed light on the key electronic features of guanine and adenine binding of cisplatin. Detailed molecular orbital analyses on the guanidine moiety before and after platination at the N7 position revealed that platinum binding does not promote depurination, as is frequently seen with protonation and other alkylating agents that bind to the N7,<sup>52</sup> because the Pt-binding is a much more localized phenomenon and there is no electronic communication with the C9–C1' bonding orbital upon Pt binding. We showed that while the thermodynamic driving force for depurination increases in the case of both platination and protonation, the barrier for cleavage of the glycosidic bond remains essentially the same upon platination compared to the unmodified nucleotide, while it decreases by ~10 kcal mol<sup>-1</sup> when the N7-position is protonated, thus allowing for facile cleavage of the glycosidic bond, in good agreement with the observation of depurination upon protonation.

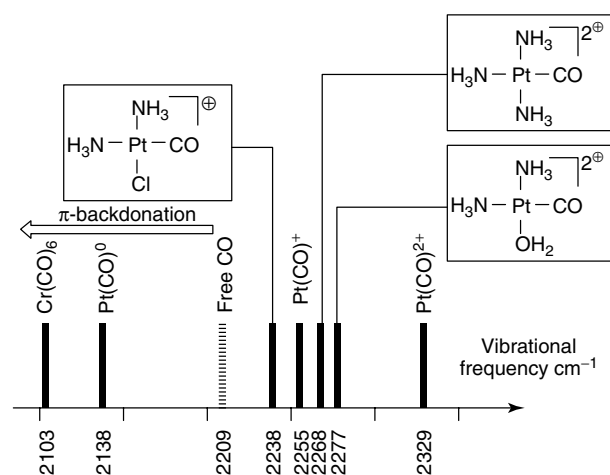
Cisplatin has been known to bind to guanine with much greater preference over adenine, which is somewhat surprising because it could be argued that the inductive effects of the electron-withdrawing oxo group at the C6 position of guanine should reduce the electron density at N7 compared to adenine that has an electron-donating amino group at the C6 position, thus making the N7 of guanine *less* nucleophilic compared to adenine. In the cisplatin system, the preference for guanine is found to be partly kinetic in origin with the transition state for binding guanine being ~5 kcal mol<sup>-1</sup> lower than the corresponding transition state for adenine binding (Figure 4a). Using the Ziegler–Rauk energy decomposition analysis, approximately 50% of this preference is attributed to a strong hydrogen bond at the transition state between one of the ammine ligands on cisplatin and the O6 of guanine.<sup>53</sup> The remaining 50% originates from an intrinsically stronger Pt–N7 bond in guanine compared to adenine, due to a greater lobe on the nitrogen N7 lone pair in guanine, resulting in better overlap with the platinum LUMO, i.e., despite the inductive effects outlined above, the N7 of guanine is more nucleophilic than that of adenine (Figure 4b). This observation can be understood intuitively by considering another major difference between adenine and guanine, namely, that N1 of



**Figure 4** Preference for binding guanine over adenine. (a) Reaction profile for the formation of monofunctional adducts with adenine and guanine. (b) Frontier MOs that participate in Pt-purine bonding. (c) Effect of N1 protonation on the size of N7 lone pair lobe. (Reproduced from Ref. 53. © ACS, 2003.)

guanine is protonated, while adenine exposes an N1 lone pair. The presence of the N1 proton diminishes the delocalization of electron density over the nitrogen lone pairs of the purine skeleton resulting in greater localization of electron density on the N3 and N7 atoms of guanine, compared to adenine where the electron density is delocalized over the N1, N3, and N7 atoms. This concept is supported by comparative calculations on tautomers of adenine and hypoxanthine, which serve as slightly simplified models of guanine (Figure 4c). The enol tautomer of hypoxanthine binds cisplatin significantly less tightly than the keto tautomer of adenine. Raber *et al.*<sup>54</sup> used similar models to explain the preference for guanine. In addition to the kinetic preference observed by Baik *et al.* favoring guanine, the authors also found a thermodynamic preference in the stability of the initial adduct of guanine compared to adenine, dominated by hydrogen bonds.

In an attempt to identify yet another subtle electronic feature that could help in distinguishing between the

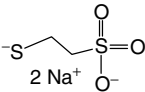


**Figure 5** Calculated vibrational stretching frequencies of C–O bonds in various platinum complexes, compared with free CO. (Reproduced from Ref. 55. © Wiley-VCH, 2003.)

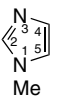
reactivity of adenine and guanine, the potential of the *cis*-diamminechloridoplatinum(II) ([Pt]) fragment to engage in  $\pi$ -backdonation was modeled using CO ligands as probes.<sup>55</sup> Because adenine and guanine have different exocyclic substituents (amine vs. carbonyl), their respective HOMOs would be expected to have different  $\pi$ -donation abilities, which would be reflected in their CO stretching frequencies. The results suggest however that the [Pt] fragment is a poor  $\pi$ -donor; thus  $\pi$ -backdonation does not appear to play a major role (Figure 5). This finding is also supported by the non-coplanar orientation of the [Pt] moiety relative to the purine plane.

As mentioned in the introduction, the use of cisplatin in chemotherapy is dose-limited due to its toxicity and

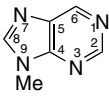
acquired resistance. In addition, less than 5% of the cisplatin entering a cell eventually forms adducts with DNA. One obvious explanation for these observations is that cisplatin binds to other cellular components, resulting in either deactivation of the drug and/or disruption of normal biochemical pathways. Thus, significant efforts have focused on understanding the binding of cisplatin with other entities found in the cells, in particular *S*- and *N*-containing ligands that are expected have the greatest affinity for platinum based on good hardness-softness matching. Deubel reported a thorough DFT study which compared the Pt-L bond strengths of a series of triammineplatinum(II) complexes with oxygen-, nitrogen- and sulfur-donor ligands as models of competing ligands encountered in a biological system (Figure 6).<sup>56</sup> The results showed

	Model complex [Pt(NH <sub>3</sub> ) <sub>3</sub> L] <sup>2+</sup>	Model ligand L =	Biological relevance
	1	H <sub>2</sub> O	H <sub>2</sub> O
	2	MeOH	ROH
	3	NH <sub>3</sub>	
	4	MeNH <sub>2</sub>	RNH <sub>2</sub>
	5	H <sub>2</sub> S	
	6	MeSH	Cysteine (Cys)
	7	Me <sub>2</sub> S	Methionine (Met)
	8	MeS <sup>-</sup> Na <sup>+</sup>	Deprotonated thiols Protecting agents, e.g., Mesna: 
	9	Melm	Histidine (His)
	10	MePur	
	11	MeA	Adenine sites of DNA
	12	MeG	Guanine sites of DNA

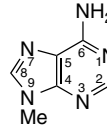
  



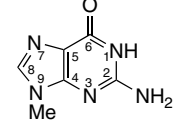
Melm



MePur



MeA



MeG

	0, L = □ <sup>b</sup>	1, H <sub>2</sub> O	2, CH <sub>3</sub> OH	3 <sup>d</sup> , NH <sub>3</sub>	4, CH <sub>3</sub> NH <sub>2</sub>	5, H <sub>2</sub> S	6, MeSH	7, Me <sub>2</sub> S	8, MeSNa	9, Melm	10, MePur	11 <sup>e</sup> , MeA	12, MeG
Pt-N <sub>α</sub>	2.092	2.085	2.083	2.094	2.094	2.098	2.096	2.099	2.084	2.086	2.090	2.084	2.067
Pt-N <sub>β</sub>	2.022	2.054	2.065	2.092	2.107	2.128	2.144	2.157	2.168	2.113	2.110	2.113	2.102
Pt-N <sub>χ</sub>	2.089	2.096	2.096	2.095	2.094	2.098	2.095	2.091	2.082	2.087	2.088	2.093	2.100
Pt-L		2.115	2.099	2.097	2.097	2.324	2.317	2.315	2.323	2.033	2.041	2.039	2.046
N <sub>α</sub> -Pt-L	86.6°	84.4	84.0	89.4	90.5	87.2	86.5	85.6	87.6	88.3	88.1	86.4	87.6
L-Pt-N <sub>χ</sub>	86.6°	92.8	93.2	90.0	90.2	93.8	94.2	95.0	88.9	88.4	88.0	89.7	90.2
ΔE	0.0	-49.4	-57.2	-71.8	-77.6	-61.9	-73.8	-83.1	-129.1	-103.5	-90.0	-94.1	-117.9

<sup>a</sup>N<sub>α</sub> and N<sub>χ</sub> are the nitrogen atoms of the ammine ligands *cis* to L; N<sub>β</sub> is the nitrogen *trans* to L. Selected structures are displayed in Figure 4. <sup>b</sup>□ = free coordination site. <sup>c</sup>Estimated by N<sub>α</sub>-Pt-N<sub>χ</sub> 173.3 deg, N<sub>α</sub>-Pt-N<sub>β</sub> 93.2 deg, N<sub>β</sub>-Pt-N<sub>χ</sub> 93.5 deg. <sup>d</sup>X-ray structure: Pt-N<sub>α</sub> 2.057; Pt-N<sub>β</sub> 2.052; Pt-N<sub>χ</sub> 2.057; Pt-L 2.052; N<sub>α</sub>-Pt-L 89.8; L-Pt-N<sub>χ</sub> 90.2. Rochon, F. D.; Melanson, R. *Acta Crystallogr.* 1980, *B36*, 691. <sup>e</sup>X-ray structure: Pt-N<sub>α</sub> 2.052; Pt-N<sub>β</sub> 2.022; Pt-N<sub>χ</sub> 2.016; Pt-L 2.000; N<sub>α</sub>-Pt-L 91.3; L-Pt-N<sub>χ</sub> 87.4; dihedral angle C8-N7-Pt-N<sub>α</sub> -107.6 (calcd 111.3). Beyer-Pfurr, R.; Jaworski, S.; Lippert, B.; Schollthorn, H.; Thewalt, U. *Inorg. Chim. Acta* 1985, 107, 217.

**Figure 6** Model complexes studied (top) and their computed geometric and thermodynamic parameters (table): Bond lengths are in angstrom, bond angles in degrees, and energies in kilocalories per mole. (Reproduced from Ref. 56. © ACS, 2002.)

that the *N*-donor ligands had the greatest binding energies; a surprising result considering that based on a purely hardness/softness argument, *S*-donors are expected to be preferred.

In another study, the kinetics of the substitution reaction of various nitrogen- and sulfur ligands with the activated cisplatin complex was modeled using DFT.<sup>57</sup> This study revealed that kinetically *N*-donor ligands were preferred over *S*-donors, with the selectivity originating from electrostatic rather than orbital-based interactions. Similarly, Zimmermann *et al.* compared the binding energies of activated cisplatin derivatives with cysteine and methionine amino acids, and showed that the binding to cysteine is much stronger than that to methionine, and nearly the same as that to guanine.<sup>58</sup> This finding was in keeping with experimental evidence, leading to the proposal that cisplatin forms reversible adducts with methionine, while irreversible binding to cysteine could be one pathway for deactivation and toxicity. The Deubel group also studied the loss of the ammine ligands of cisplatin as an inactivation pathway.<sup>59</sup> Their results showed that while the nitrogen-donor nucleobases adenine and guanine had no tendency to cause ammine loss, in case of sulfur-donor ligands, a strong trans influence promoted the loss of an ammine, thus rendering the drug inactive. In addition to the amino acids cysteine and methionine, other sulfur-containing molecules are abundant in the cell, in particular the antioxidant glutathione.

## 6 LARGE MODELS

While the small model studies were critical in understanding the key electronic features of cisplatin chemistry, larger models were needed to simulate the binding of the drug to DNA more realistically, and to elucidate the structural features of such DNA fragments. Some of the critical questions to be addressed included the degree of local bending/unwinding upon cisplatin binding, the disruption of

base stacking and other local distortions, the thermodynamics of the various possible adducts, the directional preference in the formation of the bifunctional adducts, the ineffectiveness of transplatin, the effect of cisplatin binding on the dynamics of DNA, and the binding and recognition of HMG domain and/or DNA repair proteins to these adducts.

With computing power becoming increasingly accessible, quantum mechanical methods could be applied to extended systems that include not only the *cis*-diammineplatinum(II) moiety and the purine bases to which it was bound, but also the DNA backbone, surrounding nucleotides, as well as complementary bases and strands. This allowed modeling of the drug-DNA interactions with higher accuracy than was possible by classical force fields. An example is the work by Gu *et al.*<sup>60</sup> in which the AIM analysis based on DFT was applied to study the hydrogen bonding patterns in *trans*-platinated G:C base pairs and G:C,C:G tetrads, which were compared to proton binding to the same complexes. The results show that platination reduces the intrabase hydrogen bonding in both the G:C and G:C,C:G tetrads. In the tetrad however, new hydrogen bonds between C–H5(C)···N1(G) are formed due to the geometric changes upon platination (Figure 7). While such novel hydrogen bonding is important in the development of new molecular architectures that take advantage of the structural constraints imposed by the *d*<sup>8</sup> platinum center, the large conformational flexibility of unbound nucleobases raises questions about how realistic these structural movements are for typically more constrained biological systems. Nonetheless, it is clear that hydrogen bonds are critical for understanding both the structure and energetics of cisplatin–DNA interactions and the exploration of novel patterns of hydrogen bonding networks is at the very least inspiring.

As mentioned in the introduction, the GpG crosslink is the most common adduct, followed by the ApG crosslink. Surprisingly, the GpA crosslink has never been observed in full-length DNA, prompting several computational studies in search of an explanation. One popular proposal was based on the relative distances from the N7 of a central guanine and the

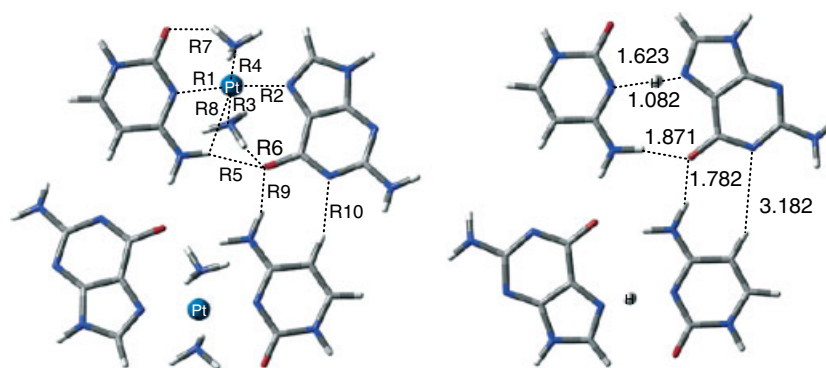


**Figure 7** Computed geometries of the GCGC tetrad bound to the *trans*-[(NH<sub>3</sub>)<sub>2</sub>Pt(II)]<sup>2+</sup> fragment and proton. (Reproduced from Ref. 60. © ACS, 2004.)

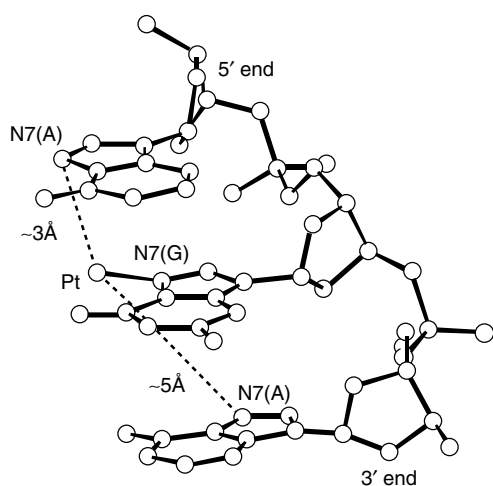


**Figure 8** Distance between platinum bound to a central guanine and the N7 atoms of the adjacent guanine bases. (Reproduced from Ref. 61. © ACS, 1984.)

N7 atoms of neighboring adenines in the 5' and 3' directions. By measuring these distances in the X-ray crystal structure of B-DNA, Dewan<sup>61</sup> showed that the N7 in the 5' direction was almost 2 Å closer than that in the 3' direction, suggesting that it was intrinsically easier to close toward the 5' direction (Figure 8). This explanation, however, assumes that there is no distortion upon formation of the initial monofunctional adduct. Moreover, 1,3-intrastrand adducts are well known, proving that much larger distances can be overcome. Thus, alternative hypotheses were needed.

Zeizinger *et al.* modeled the thermodynamics of adducts of the type BpB', where B and B' were adenine or guanine, using DFT on full models that included the bases and their sugar-phosphate backbones (Figure 9).<sup>62</sup> Comparison of the relative energies of the complexes showed that the GpG adduct indeed was the most stable complex, while the ApA complex was the least stable, in keeping with the experimental observation that ApA adducts are not seen in real DNA. Surprisingly, this study showed that the GpA adduct is more stable than the ApG adduct, in contradiction with experimental observations.

Our own work<sup>63</sup> used DFT to probe both the kinetics and thermodynamics of the platination reaction of ApG and GpA adducts to explain why the ApG adduct is preferred over GpA. In contrast to the previous study, our calculations indicated only a small thermodynamic preference for the ApG adduct, the magnitude of which was too small to account for why the GpA adducts are not observed at all. Instead, we found a strong kinetic preference for making the second Pt–N7 bond toward the 5' direction when forming the intrastrand bifunctional crosslinks. This preference was dominated by a hydrogen bonding pattern that was more favorable during closure in the 5' direction because the backbone phosphates were closer to one of the ammine ligands of cisplatin in

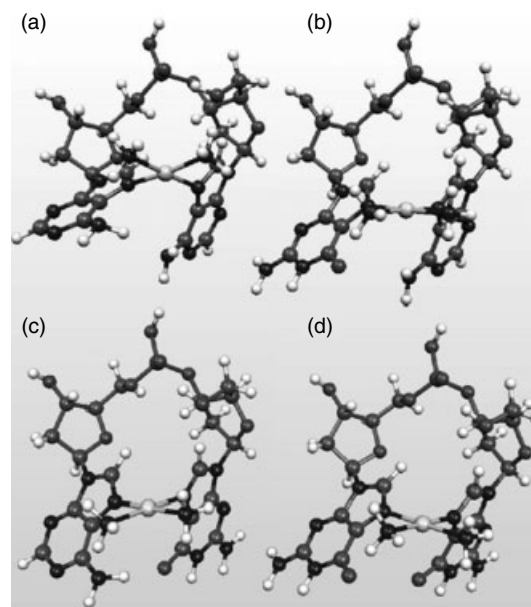


**Figure 9** Optimized geometries of the BpB' dinucleotides bound to cisplatin. (Reproduced from Ref. 62. © RSC, 2004.)

that case. As shown in Figure 10, which compares the two transition state structures, closure toward the 5' end (leading to the ApG adduct) involves hydrogen bonds with all the ligands to platinum, leading to a significant stabilization of the trigonal bipyramidal transition state for the associative ligand-exchange mechanism. Of particular importance is the axial ammine ligand, which is oriented toward the phosphate group 5' to the adenine. In contrast, in case of 3' closure to form the GpA adduct, the axial ammine ligand of cisplatin points away from the DNA-backbone and out from the DNA major groove due to the right-handedness of the DNA  $\alpha$ -helix, and is consequently not involved in any intramolecular hydrogen bonding. This exposure of the ammine group gives rise to a better solvated fragment, but the solvation energy does not fully compensate for the loss of hydrogen bonding in our simulations, leading to an overall higher transition state energy for the GpA structure.

While these large-model QM simulations allow for studying how cisplatin influences and is influenced in turn by its surrounding environment, the models still represent only a very small local portion of the real DNA. The understanding of long-range effects such as overall DNA bending, unwinding, hydration changes, the influence of the complementary strand and adduct recognition by DNA repair proteins is limited by the size of the system which makes QM methods far too expensive to be practical. Moreover, many of the large-scale effects are dynamic in nature; thus using static models raises serious concerns and may lead to misleading results due to convergence to local minima. Classical mechanics

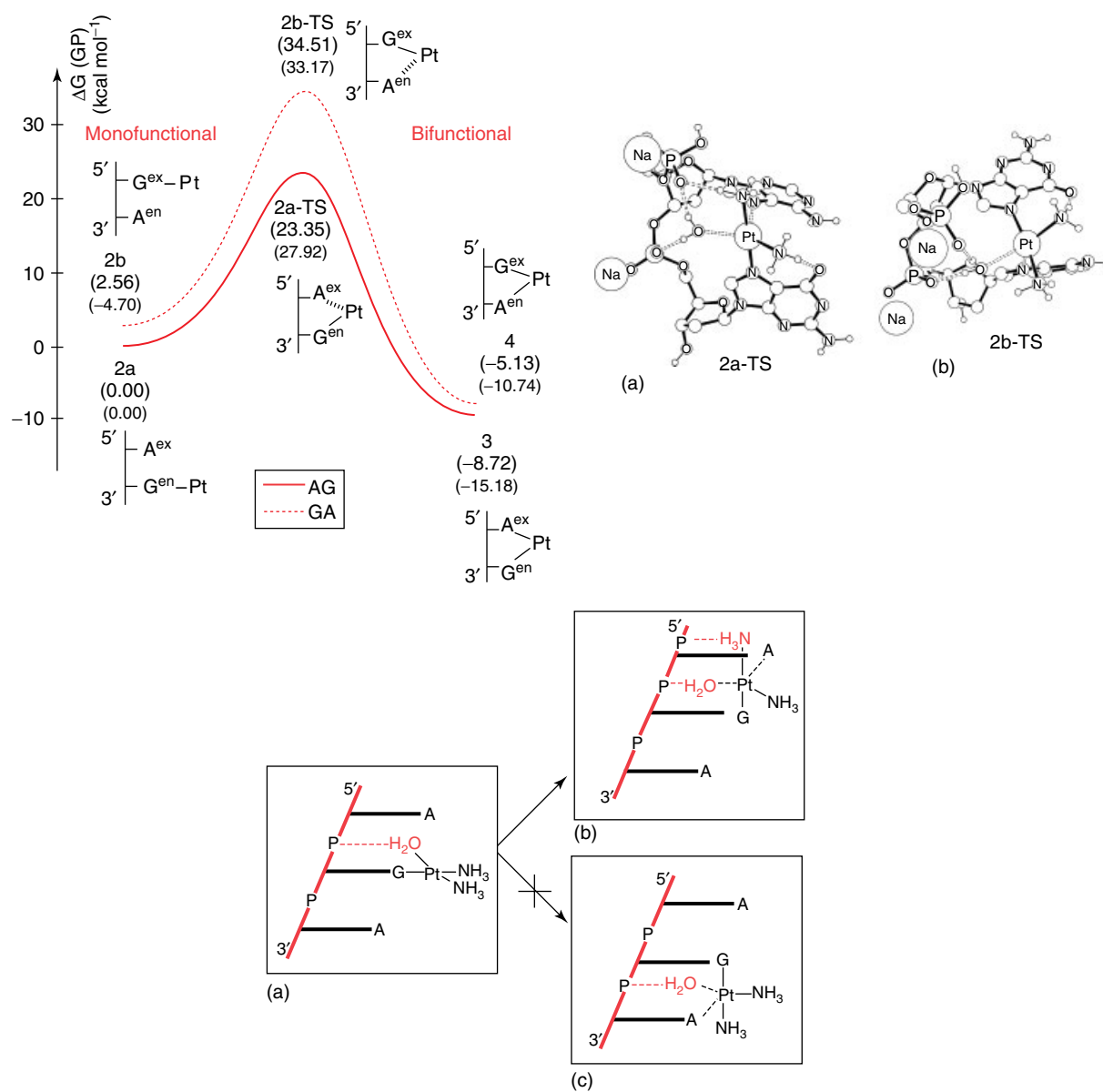


**Figure 10** Reaction free energy profile for the formation of ApG and GpA adducts with cisplatin (top, left), and the corresponding transition state structures (top, right). The cartoon at the bottom is a scheme describing the H-bonding network formed during closure in the 5' and 3' directions. (Reproduced from Ref. 63. © ACS, 2007.)

using force fields that are specifically designed for DNA-cisplatin interactions offer an attractive alternative. These can be incorporated into both classical molecular dynamics and hybrid QM/MM frameworks.

The first report of a molecular mechanics force field specifically designed for cisplatin–DNA interactions was by the Marzilli group,<sup>64</sup> who built on the foundation of the Amber nucleic-acid force-field of Kollman,<sup>65</sup> and the later improved force-field by Wilson that was specifically parameterized for DNA-cation interactions (*see Molecular Mechanics in Bioinorganic Chemistry*).<sup>66</sup> This force field was subsequently used by a number of groups to study various aspects

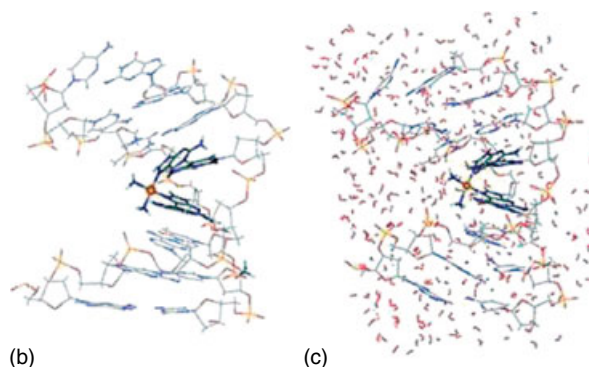
of cisplatin–DNA interactions using classical molecular mechanics and dynamics.<sup>67–72</sup> As a further enhancement in cisplatin–DNA parameterizations, Lopes *et al.* have reported on the derivation of the Lennard–Jones potentials of cisplatin in aqueous solution based on MP2 calculations.<sup>73</sup> These were then applied in a Monte Carlo simulation of cisplatin in solution, with similar results to those from CPMD simulations, in particular the nature of the hydration shells around the cisplatin unit and the distribution of hydrogen bonds to platinum and its ligands.

Several studies made use of the AIM method to better understand the effect of noncovalent interactions

	Platinated		Free	
	$E_{\text{HB}}^{(a)}$	$E_{\pi}^{(a)}$	$E_{\text{HB}}^{(a)}$	$E_{\pi}^{(a)}$
cisGpG <sub>hi</sub>	21.16	0.00	20.00	2.42
cisGpA <sub>hi</sub>	12.92	1.25	9.75	5.90
cisGpG <sub>chel</sub>	23.88	0.00	20.00	2.42
cisGpGpG <sub>hi</sub>	28.81	5.04	20.70	9.70
		(5.04+0.00) <sup>(b)</sup>		
cisGpApG <sub>hi</sub>	26.18	5.94	17.93	10.40
		(5.02+0.92) <sup>(b)</sup>		

(a) AIM estimated energy. (b) Contributions from G1...G2 & G2...G3 for cisGpGpG<sub>hi</sub> and G1...A2 & A2...G3 for cisGpApG<sub>hi</sub> in parentheses.

(a)



(b)

(c)

**Figure 11** (a) Hydrogen bonding and  $\pi$ -stacking energies of various cisplatin–DNA chelates. (b,c) Starting and optimized structures of a cisplatin–DNA adduct in explicit water. (Reproduced from Ref. 74. © Wiley-VCH, 2006.)

such as  $\pi$ -stacking and hydrogen bonds on the stabilities of biomolecules, in particular nucleic acids. This method was applied to cisplatin–DNA complexes in dinucleotide- and trinucleotide- single and double stranded models by Robertazzi *et al.*,<sup>74</sup> who incorporated an AIM analysis into a QM/MM framework (Figure 11). Geometry optimizations using QM/MM calculations at the DFT level for the QM part were followed by single point energy calculations using the BH&H functional, which had previously been shown to accurately reproduce weak interactions such as stacking and hydrogen bonding. Consistent with experimental data, this study showed that bifunctional platination in either single or double strands induces significant distortion of the helix and disruption of  $\pi$ -stacking, thereby destabilizing the structure by 3–6 kcal mol<sup>-1</sup>. On the other hand, the Watson–Crick base pairing is affected only minimally upon platination, also consistent with experimental data. In addition, several hydrogen bonds involving the cisplatin moiety are found to stabilize the DNA–cisplatin complexes.

The study of dynamical aspects of cisplatin binding in relatively large models has been possible by applying CPMD, a molecular dynamics method that uses DFT to derive the interatomic forces. In one of the first such studies, Carloni *et al.*<sup>36</sup> examined the hydrolysis of cisplatin in aqueous medium by the use of constrained MD simulations, as discussed earlier. Their estimated free energy barriers are in excellent agreement with several experimental reports, thus validating the applied protocol. The same authors also reported on the dynamics of the bifunctional GpG adduct in explicit solvent, and found the structural parameters to be in good agreement with NMR data. By combining the powerful CPMD method with a molecular mechanics framework, Spiegel *et al.*<sup>67</sup> were able to simulate even larger systems, such as a DNA dodecamer with a cisplatin adduct, and the cisplatin–DNA adduct interacting with an HMG domain protein (Figure 12). For the DNA–cisplatin complex, the starting model was based on the X-ray crystal structure of the same complex. During the simulation the structure relaxed to one that was more consistent with NMR data, thus

emphasizing the intrinsic flexibility of the system. On the other hand, the complex with HMG A is found to be far more rigid, and remains close to the crystal structure. Having thus established the reliability of this protocol, it was then applied to docking the [Pt(NH<sub>3</sub>)<sub>2</sub>]<sup>2+</sup> fragment onto DNA at the site of two adjacent guanosine moieties. Upon binding, a dramatic bend and tilt of the helix is seen, even within the short timescale of the simulation. Such a hybrid QM/MM method has been applied to several other studies of cisplatin–DNA interactions. For a comprehensive review see Ref. 75.

## 7 RELATED STUDIES

Various other studies that do not directly deal with cisplatin–DNA interactions but nevertheless contribute to our understanding of the mode of action of the drug also deserve mention. In particular, calculations comparing the electronic structure and DNA binding properties of cisplatin and second-generation Pt(II) analogs such as carboplatin, netaplatin, and oxaliplatin, as well as dinuclear Pt(II) and Pt(IV) complexes, are critical for a rational understanding of the key features involved in binding, selectivity and repair of DNA binding drugs. For example, the hydrolysis of cisplatin derivatives such as *cis*-dichloro(ethylenediamine)platinum(II) and *cis*-amminedichlorocyclohexylamineplatinum(II) (JM118) have been studied theoretically,<sup>76,77</sup> while the electronic and vibrational properties of analogs such as *cis*-diammine(oxotato)platinum(II) and 5a,6-anhydrotetracycline-platinum(II)dichloride complex were compared to those of cisplatin.<sup>78,79</sup> Classical molecular mechanics modeling of chiral antitumor agents such as *cis*-(*R,R*)-diamminecyclohexylamineplatinum(II) (oxaliplatin) and its (*S,S*)- isomer have been employed to understand the role of chirality in binding DNA.<sup>80</sup> Besides platinum, electronic structure calculations have been used to study several other anticancer compounds containing metals such as tin, ruthenium, iron, cobalt, copper etc. as well as nonmetallic complexes such as nitrogen mustards.<sup>81–83</sup>

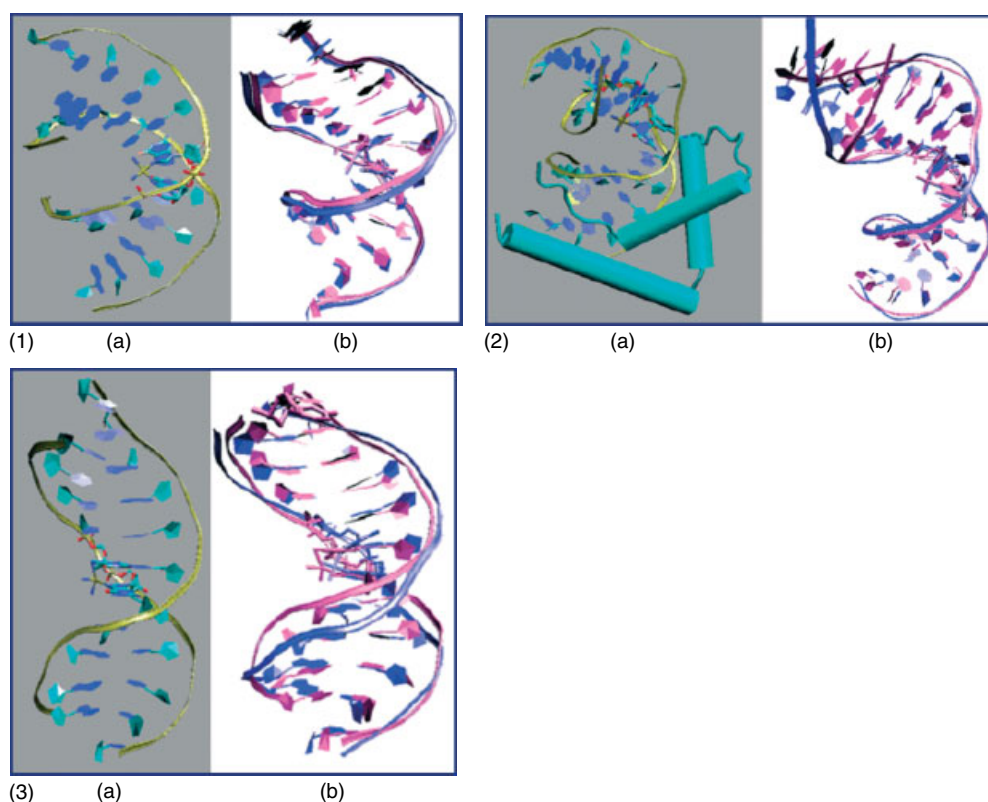


**Figure 12** Comparison between the starting (1a, 2a, 3a) and MD-averaged (1b, 2b, 3b) for cisplatin adducts with various DNA sequences. The starting structure 2a includes the HMG A domain protein bound to DNA, which is omitted in the MD-averaged structure for the sake of clarity. (Reproduced from Ref. 67. © ACS, 2004.)

From the discussion above, it is clear that computational chemistry has made and continues to make significant contributions to our understanding of drug-DNA interactions. In particular, given the challenges of studying transition metal complexes in biological environments using experimental methods, computational simulations incorporating complicated electronic structural features are an indispensable alternative. As far as cisplatin chemistry is concerned, most of the critical questions that are directly affected by the Pt(II) center, such as M–L bond energies, kinetic barriers, and local structural features, have now been addressed. What remains a challenge is capturing global structural features and interactions with other biological components that involve the formation of macromolecular tertiary complexes. The critical inter- and intramolecular forces that are likely to be operative at this scale are weak interactions such as van der Waals, stacking and other types of dispersion forces that cannot be captured to a sufficient accuracy by DFT, the current quantum mechanical method of choice. Moreover, the systems described below are far too large for purely quantum-based methods, at least in the near future, and indeed could approach the limit of classical simulation methods. Nevertheless, we present here some of the most important issues that remain to be resolved and a

handful of studies that have outlined how these challenges could be overcome.

While there are now high-resolution X-ray and NMR structures of cisplatin–DNA complexes, structural information of tertiary complexes such as NER or HMG domain proteins bound to these adducts is still challenging to obtain, both experimentally and computationally. The structural features that determine recognition of cisplatin adducts by HMG domain proteins are not fully understood, especially in comparison with other DNA binding compounds, including other Pt(II) complexes. According to the proposed mechanism of recognition based on the X-ray crystal structure of an HMG domain protein bound to cisplatin-modified DNA, HMG proteins are highly sensitive to structural distortions in DNA (Figure 13). As mentioned earlier, the formation of cisplatin adducts is accompanied by destacking of the bases and a resultant bending of the helix. The destacking allows a critical phenylalanine residue of the HMG protein to slide between two bases and stack with them from the *minor* groove side, thus providing a stable thermodynamic trap that keeps the protein bound at the site of the cisplatin adduct. Thus, there is apparently no contact of the protein with DNA from the major groove side. The differential recognition of cisplatin–DNA adducts over the others is therefore puzzling

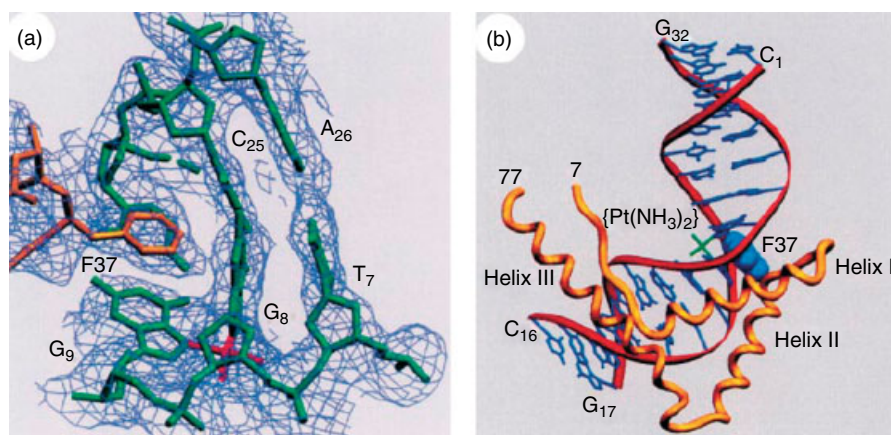


**Figure 13** X-ray crystal structure of HMG1 bound to cisplatin-modified DNA. (a)—Key phenylalanine residue of the protein shown stacked with the 3' end guanine of the GpG adduct. (b)—Overall structure of the complex. (Reproduced from Ref. 84. © Nature Publishing Group.)

because, according to the current understanding, cisplatin- and other complexes bind DNA from its major groove and cause a similar degree of bending of the helix axis. For example, the overall structural distortion caused by cisplatin and its derivative oxaliplatin are very similar based on both X-ray crystallography and NMR spectroscopy. The adducts formed by oxaliplatin ((*R,R*)-diaminocyclohexyloxalatoplatinum(II)) are, however, not recognized by HMG proteins as well as cisplatin, and are thus repaired more often. To date, there has been no attempt to use computational methods to shed light on this puzzling observation.

Similarly, it is a mystery as to why only the (*R,R*) enantiomer of the diaminocyclohexyl ligand of oxaliplatin shows significant cytotoxic activity, compared to the (*S,S*) enantiomer, when experimental studies have shown that both enantiomers have similar uptake rates and similar adducts can be formed. On the basis of the experimental structural data of the oxaliplatin-DNA adduct, an explanation has been proposed for this observation. According to this hypothesis, the equatorial proton of the (*R,R*) enantiomer of the diaminocyclohexyl ligand can form a hydrogen bond with the oxo substituent of the 3' guanine in a GpG intrastrand crosslink, while the (*S,S*) enantiomer cannot form such a hydrogen bond because that proton is now in an axial position. Molecular modeling calculations using classical force-fields have verified that the distance between the relevant proton and oxygen atom in the (*R,R*) and (*S,S*) enantiomers of platinum-bound DNA complexes is indeed larger in case of the (*S,S*) enantiomer.

A recently identified platinum complex (*cis*-diamminepyridinechloridoplatinum(II)) has only one leaving group and thus binds monofunctionally to DNA, and yet it shows promising activity as an antitumor agent,<sup>85</sup> challenging the longstanding assumption that only bifunctionally binding agents can be cisplatin analogs. That assumption, however, has been solidly founded on numerous screening tests showing that monofunctional agents were either not as efficient at

disrupting polymerase activity or were repaired at a higher rate than bifunctionally binding agents. This new compound is encouraging in that it opens up an entirely new direction for lead-compound searching, but the search is likely to be fruitless unless we understand at the molecular level what makes this compound different from the previously screened monofunctional complexes. It is plausible that the activity of this compound arises from evading the repair process, and large scale MD or hybrid QM/MM simulations are needed to address this question from a computational viewpoint (*see Quantum Mechanical/Molecular Mechanical (QM/MM) Methods and Applications in Bioinorganic Chemistry; Modeling Metalloenzymes with Density Functional and Mixed Quantum Mechanical/Molecular Mechanical (QM/MM) Calculations: Progress and Challenges*).

Many questions in the general area of DNA-binding metallodrugs remain unanswered to date. For redox-active complexes of iron, cobalt, copper etc. whose cytotoxic activity arises not from interruption of polymerase activity, but direct or indirect cleavage (via the activation of dioxygen) of the DNA backbone, pure quantum mechanical or hybrid QM/MM methods can offer critical mechanistic insights. Ab initio methods that can incorporate excited states can be applied to study the class of photoactivated DNA cleaving agents that are the main targets in photodynamic chemotherapy.<sup>86</sup> Recently, a novel binding mode of a dirhodium anticancer complex was discovered using quantum mechanical calculations,<sup>87</sup> involving bidentate binding to the N7 and C6-oxo of the same guanine.

## 8 CONCLUDING REMARKS

As summarized above, computational models have made significant contributions to understanding the nature

and reactivity of cisplatin and allowed for delineating many features of how it binds to DNA. The sophistication of the computer models has been substantially improved over the years establishing a solid foundation for future explorations of more demanding and complex questions. Perhaps, the most pressing challenge derives from the unfortunate fact that the higher precision of the model chemistry has thus far not afforded a viable novel strategy toward improving the drug or identifying a lead for the next generation of Pt-based drugs. In that regard, the majority of the work in the past has been fundamental, and this is a necessary step for computational chemistry becoming an equal partner to more traditional experimental approaches. There is growing evidence and widespread acknowledgement that a tight and irreversible Pt-DNA binding is only one of many requirements for a potent drug. Equally important is protecting the lesion against cellular repair mechanisms, such as excision repair that is believed to be connected to recognition by the HMG proteins. Both the experimental and computational base of knowledge in these new areas of research is limited and must be addressed more thoroughly in the future. To address these questions, the computer models will have to increase substantially in complexity and size to not only include a larger fragment of the DNA, but also incorporate a meaningful portion, if not the entire, HMG protein. These models will remain out of reach for purely quantum mechanical methods for some time and require carefully designed mixed models that embrace dynamic effects to properly treat the intrinsic flexibility of proteins. In addition to the conceptual challenges, many technical problems must be overcome for such models to become helpful—some of the first attempts in this direction that we have summarized above are very encouraging and illustrate the feasibility of these studies.

## 9 ABBREVIATIONS AND ACRONYMS

AIM = atoms-in-molecules; CPMD = Car-Parri-nello molecular dynamics; DFT = density functional theory; ECP = effective core potential; HMG = high mobility group; MD = molecular dynamics; MM = molecular mechanics; NER = nucleotide excision repair; QM = quantum mechanics.

## 10 REFERENCES

- G. J. Bosl, D. F. Bajorin, J. Sheinfeld, and R. Motzer, *Cancer of the Testis*, in 'Cancer: Principles and Practice of Oncology', 6th edition, eds. V. T. DeVita, S. Hellman, and S. A. Rosenberg, Lippincott, Williams & Wilkins, Philadelphia, PA, 2000.
- H. M. Pinedo and J. H. Schornagel, 'Platinum and other Metal Coordination Compounds in Cancer Chemotherapy', Plenum Press, New York, 1996.
- B. Rosenberg, L. Van Camp, J. E. Trosko, and V. H. Mansour, *Nature*, 1969, **222**, 385.
- D. Wang and S. J. Lippard, *Nat. Rev. Drug Discov.*, 2005, **4**, 307.
- B. Rosenberg, L. Van Camp, and T. Krigas, *Nature*, 1965, **205**, 698.
- B. Rosenberg, L. Van Camp, E. B. Grimley, and A. J. Thomson, *J. Biol. Chem.*, 1967, **242**, 1347.
- B. Rosenberg, E. C. Renshaw, L. Van Camp, J. Hartwick, and J. Drobnik, *J. Bacteriol.*, 1967, **93**, 716.
- S. E. Sherman and S. J. Lippard, *Chem. Rev.*, 1987, **87**, 1153.
- E. R. Jamieson and S. J. Lippard, *Chem. Rev.*, 1999, **99**, 2467.
- R. S. Go and A. A. Adjei, *J. Clin. Oncol.*, 1999, **17**, 409.
- M. A. Fuertes, C. Alonso, and J. M. Perez, *Chem. Rev.*, 2003, **103**, 645.
- S. Akiyama, Z. S. Chen, T. Sumizawa, and T. Furukawa, *Anti-Cancer Drug Des.*, 1999, **14**, 143.
- E. Wong and C. M. Giandomenico, *Chem. Rev.*, 1999, **99**, 2451.
- I. Judson and L. R. Kelland, *Drugs*, 2000, **59**, 29.
- J. Reedijk, *Chem. Commun.* 1996, (7), 801.
- D. Lebwohl and R. Canetta, *Eur. J. Cancer*, 1998, **34**, 1522.
- B. Spingler, D. A. Whittington, and S. J. Lippard, *Inorg. Chem.*, 2001, **40**, 5596.
- S. Ishida, J. Lee, D. J. Thiele, and I. Herskowitz, *Proc. Natl. Acad. Sci. U.S.A.*, 2002, **99**, 14298.
- T. D. Tullius, H. M. Ushay, C. M. Merkel, J. P. Caradonna, and S. J. Lippard, *ACS Symp. Ser.*, 1983, **209**, 51.
- J. M. Pascoe and J. J. Roberts, *Biochem. Pharmacol.*, 1974, **23**, 1345.
- M. Akaboshi, K. Kawai, H. Maki, K. Akuta, Y. Ujeno, and T. Miyahara, *Cancer Sci.*, 1992, **83**, 522.
- H. C. Harder and B. Rosenber., *Int. J. Cancer*, 1970, **6**, 207.
- J. A. Howle and G. R. Gale, *Biochem. Pharmacol.*, 1970, **19**, 2757.
- S. E. Sherman, D. Gibson, A. H. J. Wang, and S. J. Lippard, *J. Am. Chem. Soc.*, 1988, **110**, 7368.
- B. E. Bowler and S. J. Lippard, *Biochemistry*, 1986, **25**, 3031.
- J.-M. Malinge, A. Schwartz, and M. Leng, *Nucleic Acids Res.*, 1987, **15**, 1779.
- K. Kitaura, S. Obara, and K. Morokuma, *Chem. Phys. Lett.*, 1981, **77**, 452.
- J. O. Noell and P. J. Hay, *Inorg. Chem.*, 1982, **21**, 14.
- H. Basch, M. Krauss, W. J. Stevens, and D. Cohen, *Inorg. Chem.*, 1985, **24**, 3313.
- H. Basch, M. Krauss, W. J. Stevens, and D. Cohen, *Inorg. Chem.*, 1986, **25**, 684.

31. P. Carloni, W. Andreoni, J. Hutter, A. Curioni, P. Giannozzi, and M. Parrinello, *Chem. Phys. Lett.*, 1995, **234**, 50.
32. E. Tornaghi, W. Andreoni, P. Carloni, J. Hutter, and M. Parrinello, *Chem. Phys. Lett.*, 1995, **246**, 469.
33. P. N. V. Pavankumar, P. S. S. Yao, J. D. Saxe, D. G. Reddy, and F. H. Hausheer, *J. Comput. Chem.*, 1999, **20**, 365.
34. R. Wysokinski and D. Michalska, *J. Comput. Chem.*, 2001, **22**, 901.
35. G. S. Nikolov, N. Trendafilova, H. Schönemberger, R. Gust, J. Kritzenberger, and H. Yersin, *Inorg. Chim. Acta*, 1994, **217**, 159.
36. P. Carloni, M. Sprik, and W. Andreoni, *J. Phys. Chem. B*, 2000, **104**, 823.
37. J. V. Burda and M. Z. Jerzy Leszczynski, *J. Comput. Chem.*, 2005, **26**, 907.
38. J. V. Burda, M. Zeizinger, and J. Leszczynski, *J. Chem. Phys.*, 2004, **120**, 1253.
39. N. Zeizinger, J. V. Burda, J. Sponer, V. Kapsa, and J. Leszczynski, *J. Phys. Chem. A*, 2001, **105**, 8086.
40. J. V. Burda, M. Zeizinger, J. Sponer, and J. Leszczynski, *J. Chem. Phys.*, 2000, **113**, 2224.
41. Y. Zhang, Z. J. Guo, and X. Z. You, *J. Am. Chem. Soc.*, 2001, **123**, 9378.
42. J. K.-C. Lau and D. V. Deubel, *J. Chem. Theor. Comput.*, 2006, **2**, 103.
43. A. Robertazzi and J. A. Platts, *J. Comput. Chem.*, 2004, **25**, 1060.
44. J. E. Sponer, F. Glahe, J. Leszczynski, B. Lippert, and J. Sponer, *J. Phys. Chem. B*, 2001, **105**, 12171.
45. J. Cooper and T. Ziegler, *Inorg. Chem.*, 2002, **41**, 6614.
46. A. Hofmann, D. Jaganyi, O. Q. Munro, G. Liehr, and R. van Eldik, *Inorg. Chem.*, 2003, **42**, 1688.
47. J. V. Burda, J. Sponer, and J. Leszczynski, *Phys. Chem. Chem. Phys.*, 2001, **3**, 4404.
48. K. Cochran, G. Forde, G. A. Hill, L. Gorb, and J. Leszczynski, *Struct. Chem.*, 2002, **13**, 133.
49. J. V. Burda and J. Leszczynski, *Inorg. Chem.*, 2003, **42**, 7162.
50. M. Pavelka and J. Burda, *J. Mol. Model.*, 2007, **13**, 367.
51. A. Robertazzi and J. A. Platts, *Inorg. Chem.*, 2005, **44**, 267.
52. M. H. Baik, R. A. Friesner, and S. J. Lippard, *J. Am. Chem. Soc.*, 2002, **124**, 4495.
53. M. H. Baik, R. A. Friesner, and S. J. Lippard, *J. Am. Chem. Soc.*, 2003, **125**, 14082.
54. J. Raber, C. Zhu, and L. A. Eriksson, *J. Phys. Chem. B*, 2005, **109**, 11006.
55. M. H. Baik, R. A. Friesner, and S. J. Lippard, *Inorg. Chem.*, 2003, **42**, 8615.
56. D. V. Deubel, *J. Am. Chem. Soc.*, 2002, **124**, 5834.
57. D. V. Deubel, *J. Am. Chem. Soc.*, 2004, **126**, 5999.
58. T. Zimmermann, M. Zeizinger, and J. V. Burda, *J. Inorg. Biochem.*, 2005, **99**, 2184.
59. J. K.-C. Lau and D. V. Deubel, *Chem. — Eur. J.*, 2005, **11**, 2849.
60. J. Gu, J. Wang, and J. Leszczynski, *J. Am. Chem. Soc.*, 2004, **126**, 12651.
61. J. C. Dewan, *J. Am. Chem. Soc.*, 1984, **106**, 7239.
62. M. Zeizinger, J. V. Burda, and J. Leszczynski, *J. Phys. Chem. Chem. Phys.*, 2004, **6**, 3585.
63. Y. Mantri, S. J. Lippard, and M.-H. Baik, *J. Am. Chem. Soc.*, 2007, **129**, 5023.
64. S. Yao, J. P. Plataras, and L. G. Marzilli, *Inorg. Chem.*, 1994, **33**, 6061.
65. D. A. Pearlman, D. A. Case, J. W. Caldwell, W. S. Ross, T. E. Cheatham, S. DeBolt, D. Ferguson, G. Seibel, and P. Kollman, *Comput. Phys. Commun.*, 1995, **91**, 1.
66. J. M. Veal and W. D. Wilson, *J. Biomol. Struct. Dyn.*, 1991, **8**, 1119.
67. K. Spiegel, U. Rothlisberger, and P. Carloni, *J. Phys. Chem. B*, 2004, **108**, 2699.
68. S. T. Sullivan, A. Ciccarese, F. P. Fanizzi, and L. G. Marzilli, *J. Am. Chem. Soc.*, 2001, **123**, 9345.
69. L. G. Marzilli, J. S. Saad, Z. Kuklennyik, K. A. Keating, and Y. H. Xu, *J. Am. Chem. Soc.*, 2001, **123**, 2764.
70. T. W. Hambley and A. R. Jones, *Coord. Chem. Rev.*, 2001, **212**, 35.
71. S. T. Sullivan, A. Ciccarese, F. P. Fanizzi, and L. G. Marzilli, *Inorg. Chem.*, 2001, **40**, 455.
72. E. D. Scheeff, J. M. Briggs, and S. B. Howell, *Mol. Pharmacol.*, 1999, **56**, 633.
73. J. F. Lopes, V. S. D. Menezes, H. A. Duarte, W. R. Rocha, W. B. De Almeida, and H. F. Dos Santos, *J. Phys. Chem. B*, 2006, **110**, 12047.
74. J. A. P. Arturo Robertazzi, *Chem. — Eur. J.*, 2006, **12**, 5747.
75. K. Spiegel and A. Magistrato, *Org. Biomol. Chem.*, 2006, **4**, 2507.
76. L. A. S. Costa, W. R. Rocha, W. B. De Almeida, and H. F. D. Santos, *J. Chem. Phys.*, 2003, **118**, 10584.
77. C. Zhu, J. Raber, and L. A. Eriksson, *J. Phys. Chem. B*, 2005, **109**, 12195.
78. R. Wysokinski, K. Hernik, R. Szostak, and D. Michalska, *Chem. Phys.*, 2007, **333**, 37.
79. H. F. Dos Santos, B. L. Marcial, C. F. De Miranda, L. A. S. Costa, and W. B. De Almeida, *J. Inorg. Biochem.*, 2006, **100**, 1594.
80. O. Delalande, J. Malina, V. Brabec, and J. Kozelka, *Biophys. J.*, 2005, **88**, 4159.
81. H. Chojnacki, *J. Mol. Struct.: THEOCHEM WATOC '02 Special Issue*, 2003, **630**, 291.
82. X. W. Liu, J. Li, H. Deng, K. C. Zheng, Z. W. Mao, and L. N. Ji, *Inorg. Chim. Acta*, 2005, **358**, 3311.
83. J. Chen, L. Chen, S. Liao, K. Zheng, L. Ji, *Dalton Trans.* 2007, (32), 3507.

84. U. M. Ohndorf, M. A. Rould, Q. He, C. O. Pabo, and S. J. Lippard, *Nature*, 1999, **399**, 708.
85. K. S. Lovejoy, R. C. Todd, S. Zhang, M. S. McCormick, J. A. D'Aquino, J. T. Reardon, A. Sancar, K. M. Giacomini, and S. J. Lippard, *Proc. Natl. Acad. Sci. U.S.A.*, 2008, **105**, 8902.
86. L. J. Boerner and J. M. Zaleski, *Curr. Opin. Chem. Biol.*, 2005, **9**, 135.
87. D. V. Deubel, H. T. Chifotides, *Chem. Commun.* 2007, (33), 3438.